Stony Brook University

OFFICIAL COPY

The official electronic file of this thesis or dissertation is maintained by the University Libraries on behalf of The Graduate School at Stony Brook University.

© All Rights Reserved by Author.

Functional Analysis of Human Sts-2 and Sts-2 Mutants Derived from Vitiligo Patients

A Thesis Presented

by

Liucong Ling

to

The Graduate School

in Partial Fulfillment of the

Requirements

for the Degree of

Master of Science

in

Biochemistry and Cell Biology

Stony Brook University

December 2012

Stony Brook University

The Graduate School

Liucong Ling

We, the thesis committee for the above candidate for the

Master of Science degree, hereby recommend

acceptance of this thesis.

Nicholas Carpino – Thesis Advisor
Associate Professor, Department of Molecular Genetics and Microbiology

Laurie Krug – Second Reader
Assistant Professor, Department of Molecular Genetics and Microbiology

This thesis is accepted by the Graduate School

Charles Taber
Interim Dean of the Graduate School

Abstract of the Thesis

Functional Analysis of Human Sts-2 and Sts-2 Mutants Derived from Vitiligo Patients

by

Liucong Ling

Master of Science

in

Biochemistry and Cell Biology

Stony Brook University

2012

The purpose of this study was twofold: firstly, to investigate the functional differences between the short and long isoforms of human Sts-2, and secondly to identify functional consequences of specific mutations within the human T cell signaling protein Sts-2 (hSts-2). The mutations are associated with generalized vitiligo, an autoimmune disease affecting 0.5-2% population. Sts-2 exists in two forms, a short form containing 623 amino acids and a longer splice variant form containing 661 amino acids. Because two forms of hSts-2 exist, the effect of mutations in both forms was investigated. Short form hSts-2 was found to express at much higher levels than long form hSts-2. However, the mutations were found to have no effect on expression levels in 293T cells. Phosphatase assays were performed to investigate the effects of mutations on phosphatase activity. While both wild-type hSts-2 isoforms have lower phosphatase activity toward the artificial substrate OMFP than mouse Sts-2 *in vitro*, no obvious differences in the phosphatase activity of the different mutants was evident. To investigate the effects of the mutations on TCR signaling pathways, an NFAT luciferase reporter gene system was used. The luciferase assay results suggest that long form and short form hSts2 may play different roles in TCR signaling. Specifically, over-expressing long form hSts-2 results in down-regulation of the NFAT signal and over-expressing short form results in up-regulation of NFAT activation levels. However, no obvious differences were observed among long form and short form mutants, but results are inconclusive and the function of hSts-2 vitiligo-associated mutants needs to be further investigated.

Table of Contents

List of Figures

List of Abbreviations

Sts	Suppressor of TCR Signaling
Sts-2	Suppressor of TCR Signaling 2
hSts-2	Human Suppressor of TCR Signaling
mSts	Murine Suppressor of TCR Signaling
hSts-2l	Human Suppressor of TCR Signaling Long Form
hSts-2s	Human Suppressor of TCR Signaling Short Form
TULA	T-cell Ubiquitin LigAnd
NFAT	Nuclear Factor of Activated T-Cells
TCR	T Cell Receptor
CD	Cluster of Differnetiation
MHC	Major Histocompatibility Complex
APC	Antigen Present Cell
ITAM	Immunoreceptor Tyrosine-Based Activation Motif
ZAP-70	Zeta-Chain-Associated Protein Kinase 70
SMAC	Supramolecular Activating Cluster
LFA-1	Lymphocyte Function-Associated Antigen 1
ERM	Ezrin/Radixin/Moesin
IL-2	Interleukin 2
AP-1	Activator Protein 1
NF-κB	Nuclear Factor Kappa-Light-Chain-Enhancer of Activated B Cells
SLP-76	SH2 Domain Containing Leukocyte Protein of 76kDa
PLC- γ1	Phospholipase C γ1
LAT	Linker of Activated T cells
PI(4,5)P2	Phosphatidylinositol 4,5-bisphosphate
IP_3	Inositol 1,4,5-Trisphosphate
DAG	Diglyceride
ER	Endoplasmic Reticulum
STIM	Stromal Interaction Molecule 1
RasGRP	Guanyl Nucleotide-Releasing Protein
GEF	Guanine Nucleotide Exchange Factors

PKCθ	Protein Kinase C θ
MAPK	Mitogen-Activated Protein Kinase
MAPKK	Mitogen-Activated Protein Kinase Kinase
SOS	Son of Sevenless
GRB2	Growth Factor Receptor-Bound Protein 2
PKC	Protein Kinase C
PI3K	Phosphatidylinositide 3-Kinases
IKK	IκB Kinase
MALT1	Mucosa-Associated Lymphoid Tissue Lymphoma Translocation Protein 1
NEMO	NF-κB Essential Modulator
TAK1	Transforming Growth Factor β–activated Kinase 1
IKKβ	IκB Kinase β
UBASH3B	Ubiquitin Associated and Src Homology 3 Domain Containing B
SHP1	Src Homology Region 2 Domain-Containing Phosphatase-1
Cbl	Casitas B-Lineage Lymphoma Proto-Oncogene
CTLA-4	Cytotoxic T Lymphocyte Antigen-4
PD-1	Programmed Cell Death Protein 1
PTPN22	Tyrosine-Protein Phosphatase Non-Receptor Type 22
LPP	Lipoma-Preferred Partner
IL2RA	Interleukin-2 Receptor Alpha Chain
UBASH3A	Ubiquitin Associated and Src Homology 3 Domain Containing A
C1QTNF6	Complement Component C1q and Tumor Necrosis Factor Related Protein 6
RERE	Arginine-Glutamic Acid Dipeptide Repeats
GZMB	Granzyme B
CTL	Cytotoxic T Lymphocyte
PDE	Phosphodiesterase
PGM	Phosphoglycerate Mutase
UBA	Ubiquitin-Associated
SH3	Src Homology 3
CEU	European-Derived White
OMFP	*O*-methyl fluorescein phosphate

Acknowledgement

I would like to thank my advisor Dr. Nicolas Carpino for accepting me in his group and providing me the opportunity to do research on my interesting topics. I would not accomplish my work without his guidance, suggestions, encouragement, and patience. He has also been very supportive with my life and my ideas of career choices.

I would like to acknowledge Dr. Laurie Krug for her scientific suggestions and serving as my second reader, and Dr. Nancy C. Reich for her helpful advises on my project and kindly sharing equipment.

I want to thank all the members of the Carpino group present and past: Neena Carpino, Boris San Luis, Dr. Kinga Hosszu, Ellie Ivanova, Nithya Sivaram. I want to especially thank Neena for her help with experiments, and Boris for his thoughtful ideas and discussions.

I want to thank my friends in Stony Brook and in China for their encouragement and support in my life. Lastly, I would like to especially thank my parents for their continued support and encouragement through everything I am interested in.

I. Introduction

1. Immune System and T cells

1.1 Immune System

The immune system is the physiological system that protects individuals from infecting micro-organisms or foreign substances. The early stage of the immune response is called the innate immune response, and it involves a low specificity response to infecting microbes; later, a more powerful and specific response, the adaptive immune response is responsible for recognizing and eliminating foreign antigens. Two types of immune responses are involved in the adaptive immune response. One is humoral immunity; the other one is cell-mediated immunity, which is mediated by T lymphocytes, or T cells [1]. As one of core mediators of adaptive immune response, T cells play a central role in immune system.

1.2 T Cells and T Cell Receptor (TCR) Signaling

1.2.1 T Cells

T lymphocytes originate from stem cells in fetal liver and adult bone marrow, and then migrate into the thymus. During T cell maturation, sequences of genes that encode the T cell receptor (TCR) are rearranged. Two classes of T cells are differentiated at the end of development in thymus, one of which is cytotoxic T cells carrying the CD8 surface molecule and the other one is helper T cells carrying CD4 [1-2]. Then, CD8 T cells and CD4 T cells traverse through the blood either to lymphoid organs or to peripheral non-lymphoid tissues where they can be activated by major histocompatibility complex (MHC) I or MHC II receptors on mature dendritic cells or antigen present cells (APCs). Once antigen-specific T cells are activated, they proliferate and are influenced by a variety of signals to differentiate into effector cells and memory cells. Effector CD4 T cells are responsible for activation of macrophages, B cells and other cells, whereas effector CD8 T cells are for killing of infected target cells. The responses decline during a return to immune homeostasis as the antigen is eliminated [1].

1.2.2 TCR Upstream Signaling

The T cell receptor is a large multi-protein complex consisting of a disulfide-linked α/β dimer that is generated by gene rearrangement and engaged by antigen during T cell activation, and CD3 complexes existing as γε, δε, and ζζ dimers noncovalently associated with αβ heterodimer [2-3]. To initiate TCR signaling, the αβ dimer is engaged by the contact between the MHC complex and the TCR. The engagement results in phosphorylation of ITAMs on the CD3

and ζ chains by Src family tyrosine kinase Lck and Fyn. This allows recruitment to the receptor complex of the kinase ZAP-70, an essential kinase for triggering downstream signaling cascades. Phosphorylation of the transmembrane adapter protein linker (LAT) and the cytosolic adapter protein SLP-76 by activated ZAP-70 initiates the assembly of a multi-molecular complex that propagates multiple signaling pathways [4]. Following LAT and SLP-76 phosphorylation, PLC-γ1 is recruited to the membrane by binding to SLP-76, Vav1 and LAT, and phosphorylated by IL2-inducible T-cell kinase (Itk). Hydrolysis of PI(4,5)P2 by active PLC-γ1 generates IP_3 and DAG, two secondary messengers that subsequently activate transcription factors through distinct signaling pathways. One of the most important cytokines produced during this stage is interleukin 2 (IL-2), a cytokine whose transcription is regulated by activation of the transcription factors NFAT, AP-1, and NF-κB.

1.2.3 TCR Downstream Signaling

The transcription factor NFAT is regulated through IP_3/Ca^{2+}-mediated signaling pathways. Once IP3 is generated, it binds to Ca^{2+}-permeable ion channel receptors (IP_3R) on the endoplasmic reticulum (ER) membrane, inducing the release of ER Ca^{2+} into cytoplasm. ER-resident proteins stromal interaction molecule 1 (STIM1) and STIM2 sense the decrease of Ca^{2+} in the ER, STIM1 then aggregates into small clusters in the ER membrane and colocalizes with clusters of Orail, a calcium-release-activated Ca^{2+} channel protein in the plasma membrane. This triggers Ca^{2+} influx that elevates the concentration of intracellular Ca^{2+}. The calcium-sensitive protein calmodulin bound with Ca^{2+} now is able to activate the phosphatase calcineurin, which then activates the transcription factor NFAT by dephosphorylation. This leads to the translocation of NFAT from the cytoplasm to the nucleus. In the nucleus, NFAT can cooperate with its partners including activator protein 1 (AP-1) to regulate gene expressions [8].

The transcription factor AP-1 is activated by the DAG/Ras pathway. TCR-activated DAG recruits RasGRP, one of Ras GEFs in T cells, and induces the phosphorylation of RasGRP. Active RasGRP facilitates activation of Ras into the GTP-bound state, initiating the mitogen-associated protein kinase (MAPK) phosphorylation cascade by activating MAPK kinase kinase Raf-1. Phosphorylated Raf-1 then activates MAPKKs, which in turn phosphorylates MAPK's extracellular signal-related kinase 1 (Erk1) and Erk2, resulting in the activation of the transcription factor Elk1 and subsequent activation of AP-1. Son of sevenless (SOS) is the other Ras GEF that is present in T cells and constitutively bound to GRB2. LAT recruits GRB2 during

TCR stimulation, upon which SOS facilitates the activation of Ras and downstream signaling pathways [4].

PKCθ is a member of the PKC family containing a lipid-binding domain specific for DAG. It is recruited to the plasma membrane by PLCγ1-induced DAG during TCR activation. In T cells, PKCθ is phosphorylated by Lck and PI3K-activated PDK1, following which it binds to IKK, phosphorylates Carma1, and subsequently recruits Bcl10 and MALT1 [27]. Recruited MALT1 facilitates the polyubiquitination of NEMO and activates the IKK complex by TAK1-induced phosphorylation of IKKβ, allowing for the phosphorylation and degradation of IκB. Finally, IκB-sequestered NF- κB is released and translocated into the nucleus where it activates target gene expression [27].

1.2.4 Negative Regulation of TCR Signaling

T cell negative regulators inhibit TCR signaling through phosphorylation, dephosphorylation, ubiquitination, and stimulation of inhibitory receptors [4]. Phosphorylation of Lck inhibitory tyrosine residue Y505 mediated by C-terminal Src kinase (Csk) shifts Lck into an inactive state [10]. The Cbl proteins play an important negative regulatory role via Cbl-catalyzed ubiquitination of active signaling proteins that targets them for degradation [11]. Cbl-b and c-Cbl are two major members of the Cbl family with distinct roles in negatively regulating TCR cell signaling [11]. Cbl-b, involved in the co-stimulatory receptor CD28-dependent signaling pathways, binds and ubiquitylates p85, and alters downstream signaling to induce repression of TCR signaling [9]. C-Cbl is known to inhibit the stimulation of ZAP-70 in the thymus [11]. Inhibition of TCR signaling is also mediated by up-regulation of the inhibitory receptor cytotoxic T lymphocyte antigen-4 (CTLA-4) and PD-1 and subsequent recruitment of phosphatases like SHP1 [4]. CTLA-4 is engaged by B7 on the surface of APCs' leading to the dissociation of PP2A from its tail and enhancement of the activity of TCR negative regulators Cbl-b and Rap1 [12]. Finally, down-regulation of Zap-70 by the Sts proteins also negatively regulates TCR signaling by unknown mechanisms.

2. T Cells in Vitiligo

2.1 Vitiligo

Vitiligo is a common skin pigmentation disorder resulting in chronic and progressive loss of melanocytes from the affected regions. Though the pathogenesis of vitiligo is still unclear, more and more studies support the idea that vitiligo is an autoimmune disease. Disfiguration is

one of the factors that affect a patients' life due to the appearance of white patches on the skin. In addition, vitiligo patients have increased susceptibility to other autoimmune diseases relative to non-affected persons [16-17]. Understanding the molecular mechanisms of vitiligo may lead to the development of therapeutics that could significantly improve the life quality of patients.

Previous research conducted with patients' samples compared the number and ratio of different cell types and the secretion of cytokines between patients and normal population [20-22]. Together with other studies based on cell line or mouse models, several genes were identified as candidate-genes associated with vitiligo. Recently, a genome-wide association study performed by Jin Y, *et al* identified ten genes, including *major-histocompatibility-complex class I (MHC I), MHC II, PTPN22, LPP, IL2RA, UBASH3A, C1QTNF6, RERE, GZMB*, and *TYR*, as being associated with generalized vitiligo in EUR-derived populations [16]. Most of the identified genes are involved in the regulation of immune response, a finding that is consistent with the hypothesis that the destruction of melanocytes is immune-mediated. Interestingly, both *in vivo* studies and sequencing analysis suggest that susceptibility to either vitiligo or melanoma is mutually exclusive and vitiligo-derived T cells are hyper-reactive to melanoma cells [23-24]. In addition to a host of immune-related genes, overexpression of apoptosis regulatory molecule p53 is also thought to be associated with vitiligo, perhaps through a deregulation of melanocyte apoptotic machinery [18-19].

2.2 T Cell Signaling and Vitiligo

Analysis of patients' serum or skin samples have indicated a connection between generalized vitiligo and activation of cytotoxic T lymphocytes (CTLs), including melanocyte-specific CTLs [20-21] and non-specific CTLs [22]. Among the vitiligo-associated genes identified by Jin Y, *et al*, are *PTPN22* encoding Lyp, a phosphatase that negatively regulates early TCR signaling, *IL2RA* that encodes IL2 receptor α, and *UBASH3A* that encodes the TCR negative regulator Sts-2 [26] (also called TULA [28]). The possible involvements of these genes in the etiology of vitiligo are consistent with the hypothesis that aberrantly activated cytotoxic T cells induce the apoptosis of melanocytes leading to melanocyte destruction. Understanding how small genetic variations within associated genes produce functional outcomes could lead to deciphering the link between T cell responses and the induction of vitiligo

3 Introduction of Suppressor of TCR Signaling-2 (Sts-2)

3.1 Characterization of Sts-2

Encoded by the *UBASH3A* gene, Sts-2 belongs to the Suppressor of TCR Signaling (Sts) family. In mice and humans, Sts-2 is expressed specifically in T cells localized in the thymus, spleen, and bone marrow [26, 28]. Two alternative-splicing forms of Sts-2 (Figure 1.1.) exist. The two forms differ by 38 amino acids, with the shorter form (Sts-2s) expressed to higher levels than the longer form (Sts-2l).

The Sts proteins are characterized by a unique multi-domain structure containing an N-terminal UBA domain, a central SH3 domain and a C-terminal PGM domain. The PGM domain of the Sts proteins has histidine phosphatase catalytic activity, with Sts-1 *in vitro* phosphatase activity toward artificial substrates being significantly greater than that of Sts-2. The first protein in the Sts family to be discovered and characterized was Sts-1. It was isolated during an affinity isolation screen performed with a Jak2-derived phospho-peptide [25]. Following the characterization of Sts-1, Sts-2 was identified based on its 75% homology to Sts-1 [26]. At the same time, Sts-2 was also discovered from an analysis of c-Cbl-associated proteins and designated as T-cell Ubiquitin Ligand (TULA) [28]. To date, the exact function of Sts-2 in TCR signaling is unknown, although the *Sts-1/2*$^{-/-}$ mouse model suggests that Sts-2 is a negative regulator of TCR signaling [26] because *Sts-1/2*$^{-/-}$ T cells are hypersensitive to TCR stimulation. Interestingly, however, overexpression of Sts-2 in Jurkat T cells *enhances* the activation of signaling pathways, possibly by facilitating the ubiquitination and degradation of c-Cbl [28].

A number of genome-wide association studies have linked Sts-2 to a number of autoimmune diseases, including vitiligo [16], type 1 diabetes [33], and rheumatoid arthritis [34].

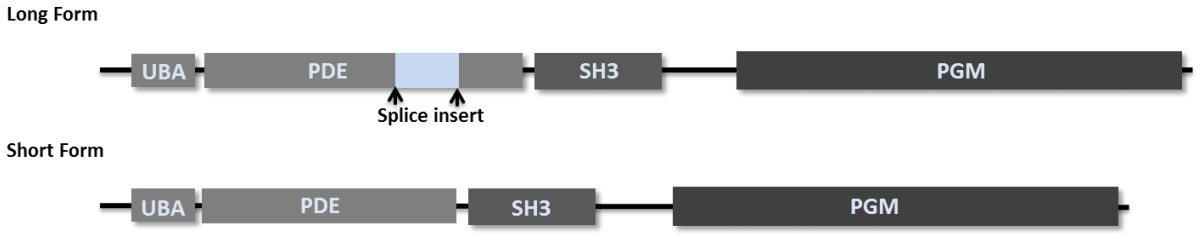

Figure 1.1: Domains and alternative splicing sites in full length human Sts-2 (hSts-2).

Multi-domains in Sts-2 include UBA, PDE, SH3 and PGM domain. Loop between SH3 domain and PGM domain is longer than others. The sequence between two black arrows is absent in short form hSts-2.

3.2 Structure of Sts-2

The N-terminal ubiquitin-associated (UBA) domain is a bundle of three α-helices with a hydrophobic core [35]. Most UBA domains bind to ubiquitin and ubiquitin-like domains via hydrophobic surface patches including a conserved methionine residue in the α1-α2 loop [35]. However, different UBA domains recognize ubiquitin differently, such as Cbl UBA domains: the Cbl-b UBA domain binds ubiquitin through α1 helix and dimerization of c-Cbl UBA domain with its α2α3 helices may be necessary for ubiquitination of its substrate [35, 39, 41]. The mechanism of Sts-2 UBA domain's interaction with ubiquitin is unclear.

The region between the UBA and SH3 domains is labeled a PDE domain based on homology with the 2H phosphoesterase super family [42]. Phosphodiesterases (PDEs) are enzymes that catalyze conversion of molecules such as ATP and GTP to cyclic adenosine monophosphate (cAMP) and cyclic guanosine monophosphate (cGMP) respectively [43]. Both cAMP and cGMP are important second messengers involved in regulation of cell cycle, cell proliferation, and cell metabolism [43]. Two conserved histidines characterize the active sites of PDE family members [42]. One of the conserved histidines in hSts-2 is His110, adjacent to Val-111, a residue that is found mutated in vitiligo patients; however, the hSts- 2 PDE activity has not been investigated yet.

Src homology 3 (SH3) domains specifically bind to proline-rich sequence via a proline-rich core binding groove and a specificity pocket leading to direct protein-protein binding [36]. The simulation of SH3 domain aggregation infers two possible aggregation conformations including the closed form dimer that forms through the exchange of two proteins' RT-loops, and the open aggregation state [37]. Sts-2 binds to c-Cbl through the SH3 domain but whether Sts-2 SH3 has additional functions is unknown.

The fourth domain in Sts-2 is C-terminal phosphoglycerate mutase (PGM) domain. PGM is also termed 2H phosphatase domain for the family members dephosphorylate substrates by two catalytic histidine residues. The first His residue is the nucleophilic residue belonging to the RHGE motif; and the second one stabilizes the nucleophilic attack with two conserved Arg residues [38]. It has been confirmed that the PGM domain in Sts-2 has phosphatase activity regulated by its 2H residues His336 and His551 with conserved Arg365 and Arg448 residues [30] (residues refer to short form). The PGM domain also mediates dimerization of Sts-2 [32].

3.3 Sts-2 Mutants Derived From Generalized Vitiligo Patients

The identification of a variety of mutations within Sts-2 that are associated with the disease vitiligo was published by Jin, Y. *et al*. (2010). The study described genome-wide sequencing on 1514 generalized vitiligo patients who were of European-derived white (CEU) ancestry [16]. The SNPs found in those patients were compared with 2813 CEU controls and were considered as statistically significant association if P values were less than 0.05 [16]. Five variants in the region of *Sts-2* on chromosome 21q22.3 were identified at the amino acid level as S18G, S18G-L28F, S18G-V111M, S18G-V111M-R324Q, and S18G-D466E (number refer to long form). The functional analysis of Sts-2 isoforms and vitiligo-associated mutants will be discussed herein. With the exception of the S18G mutation, the remaining four point-mutations are distributed in the four domains of hSts-2 respectively (Figure 1.2).

The first domain in Sts-2 is UBA domain and has been confirmed to have ubiquitin binding activity [32]. Multiple alignments based on UBA protein family seeds indicate that Leu-28 in Sts-2 is a highly conserved residue; over 70% proteins in UBA family have leucine in this position (Figure 1.3). Together with other highly conserved residues inside the UBA domain, Leu-28 could be important for maintaining the structure of the three α-helixal bundles through its interactions with other hydrophobic residues such as leucine, valine, and alanine (Figure1.4). The L28F mutation could disrupt the stability of the UBA structure.

The second domain in Sts-2 has not been confirmed, although it is referred to as a phosphodiesterase (PDE) domain based on homology to putative family members [42] (Figure 1.2a). Within homologues, a valine or isoleucine is generally found at this position. Interestingly, the residue that precedes Val-111 is one of the histidines that is considered to play a critical role in catalytic activity. Thus, the V111M mutation might affect either PDE catalytic activity or, more likely, the interactions of substrates within the active site.

In order to gain more insight into the possible effects of the R324Q mutation within the SH3 domain, multiple SH3 domains were aligned with the hSts-2 SH3 domain. The third SH3 domain of Sorbs-1 was identified as the most similar to the Sts-2 SH3 domain. Ribon V. *et al* have confirmed that Sorbs-1, also called c-Cbl binding protein, binds to c-Cbl through the interaction between its third SH3 domain and poly-proline motif in c-Cbl [13]. The structure of Sorb-1, therefore, is used as a representative structure indicating the location of the mutation site relative to the ligand-binding region. Sts-2 Arg-324 is located on the opposite side of the ligand binding site, exposed on the surface (Figure 1.5). Therefore, instead of affecting ligand binding,

the mutation site may help to recruit other proteins or form intramolecular interactions that stabilize the full length protein.

The Sts PGM domain is the most well-defined structure in Sts protein family. Based on the crystal structure of the Sts-2 PGM domain, the mutation site is on the opposite side of the molecule relative to the catalytic motif (Figure 1.6). The homologous residue is conserved as glutamine among mouse Sts-1, human Sts-1 and mouse Sts-2. In hSts-2 the aspartic acid at this position 466 is altered to a glutamate in some vitiligo patients (Figure 1.2c). This allele within the PGM domain may alter the interaction of the PGM domain with other regions of full-length Sts-2 or it might be important for maintaining the structural integrity of the PGM domain.

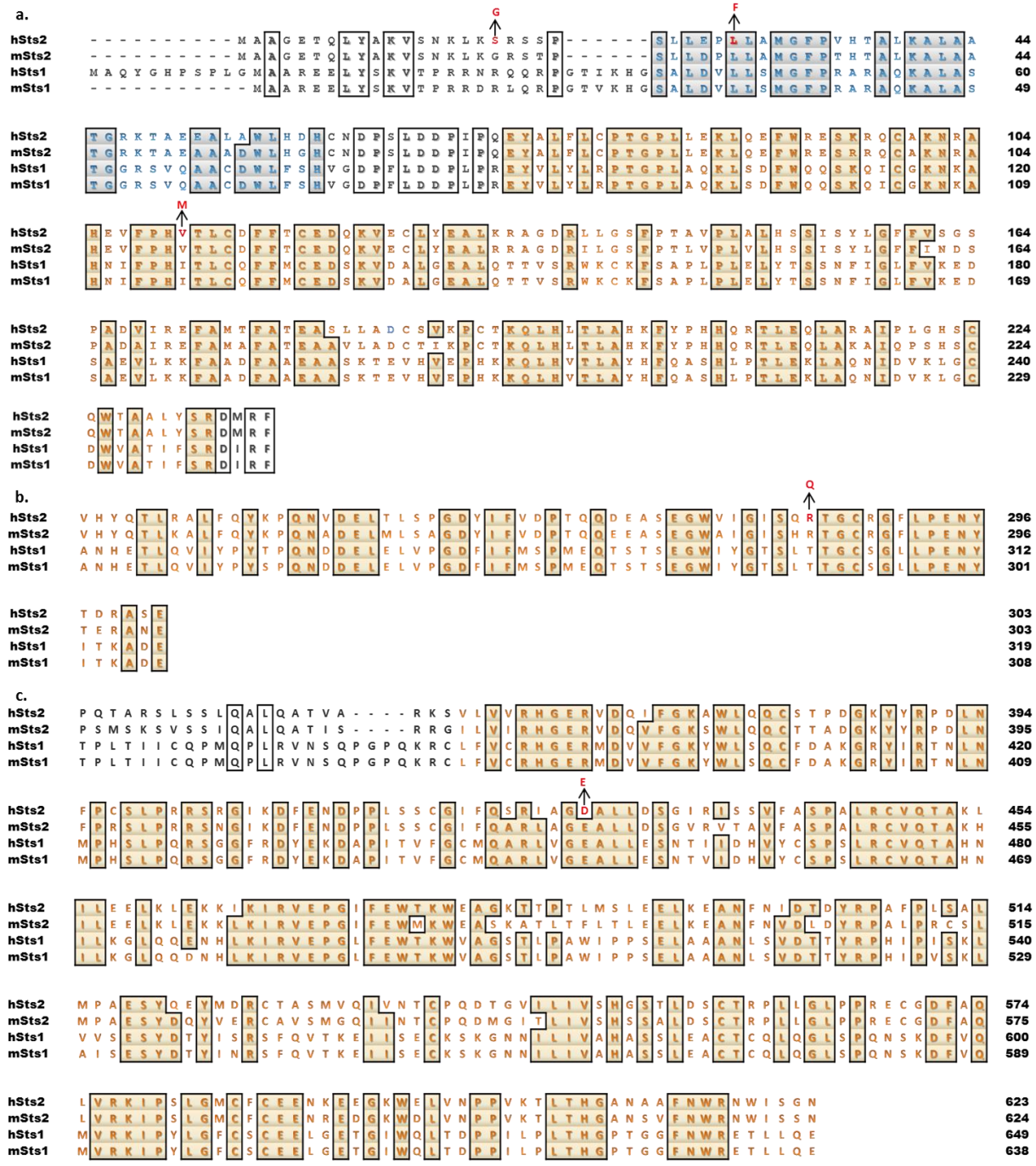

Figure 1.2: Multiple alignments of Sts proteins.

Multiple alignments were calculated by ClustalX 2.1. Vitiligo-associated mutation residues are labeled in red font. (a) Multiple alignments of UBA and PDE domain. (b) Multiple alignments of SH3 domain. (c) Multiple alignments of PGM domain.

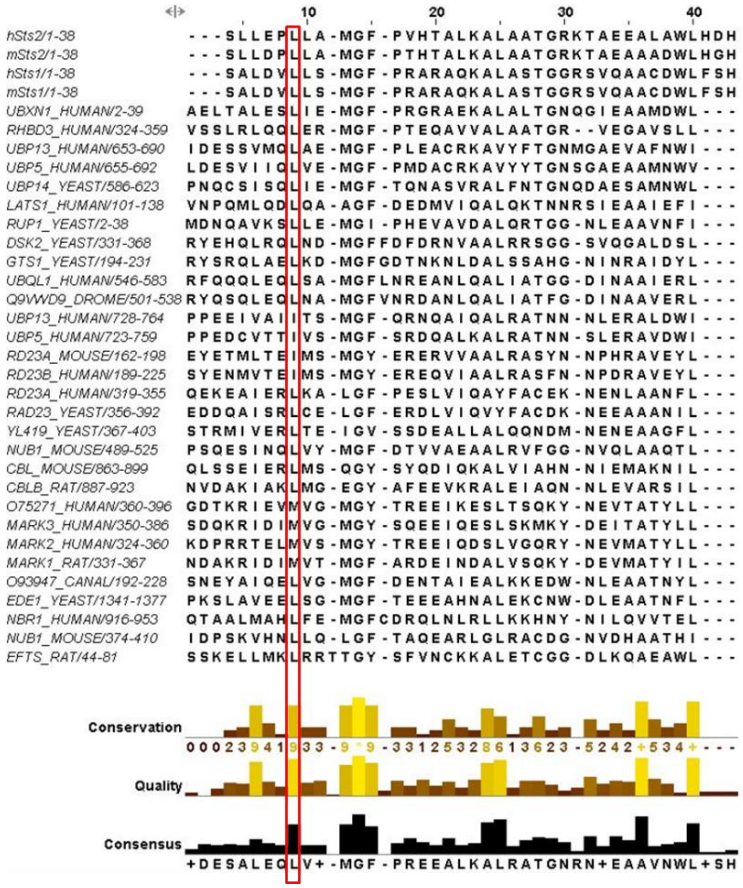

Figure 1.3: Multiple alignments of UBA family members.

Multiple alignments were calculated by ClustalX 2.1 and read out by Java™ 6. Vitiligo-associated mutation L28F is highlighted in red box showing that the residue is highly conserved among UBA family members.

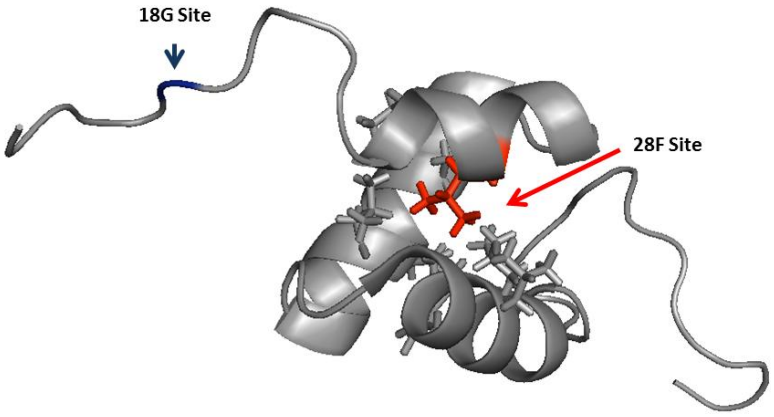

Figure 1.4: Structure of Sts-2 UBA domain.

Blue arrow indicates the presumed 18G mutation site. The location of Leu-28 residue is indicated by red arrow. Leu-28 and other conserved residues form a hydrophobic core.

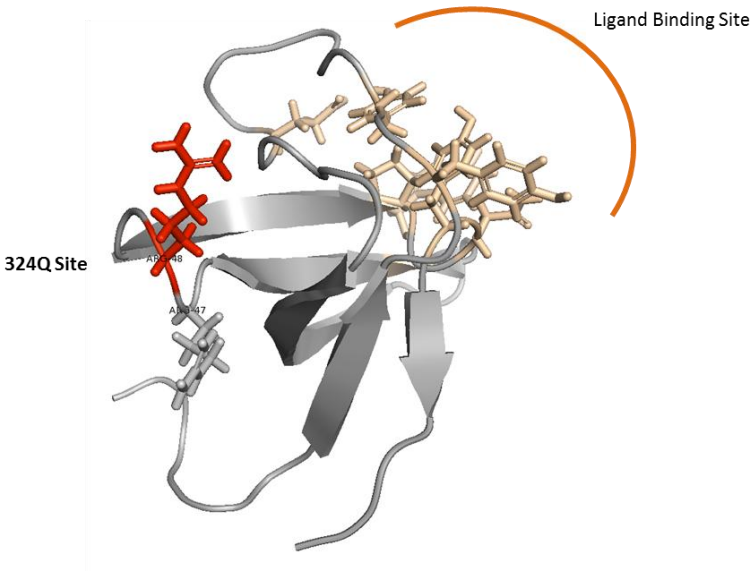

Figure 1.5: Arg324 in SH3 domain.

The structure is from Cap 3rd SH3 domain (PDB 2JL0) with 50% identity to hSts-2 SH3 domain. The side chain sticks in red represent Arg48 in Cap 3rd SH3 domain and Arg324 in hSts-2. The poly-proline binding motif (shown in yellow) is on the opposite side of the domain from Arg-48.

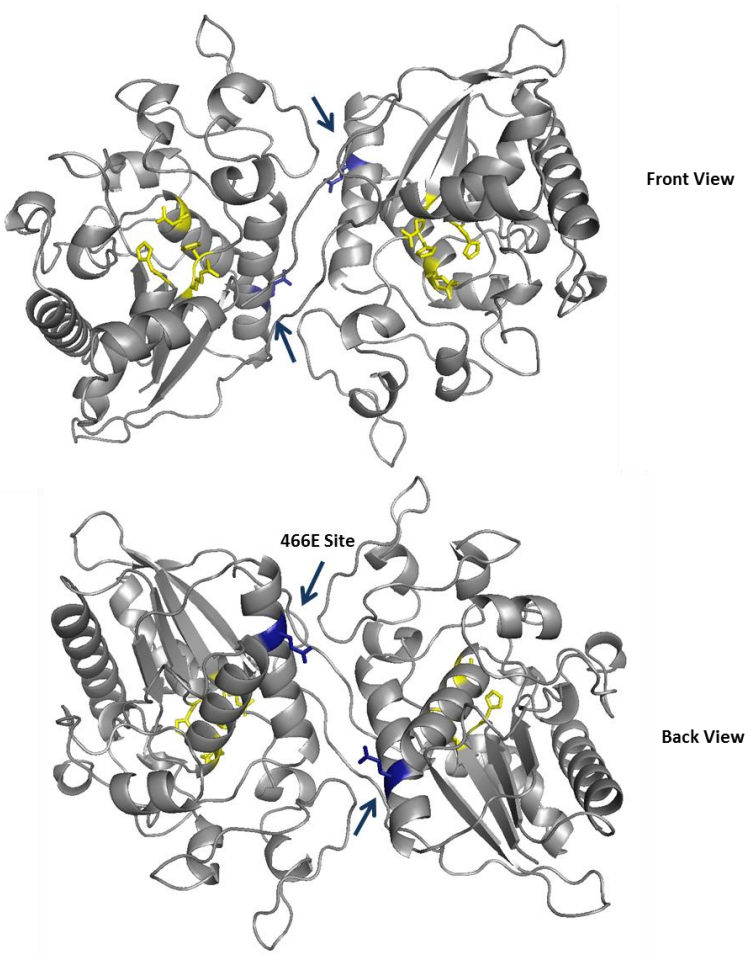

Figure 1.6: Dimerized Sts-2 PGM domain.

The structure of Sts-2 PGM domain was determined in dimers. The side chain sticks in yellow are the 2H catalytic residues. The blue arrows point the location of Asp-466 on the opposite face from the catalytic residues.

II. Materials and Methods

2.1 Bioinformatics and Data Analysis

The sequence data for multiple alignments was either from the website: pfam.sanger.ac.uk or Blast. Multiple alignments were performed by ClustalX 2.1 and read out by Java™ 6 (ORACLE). The protein structure data was from Protein Data Bank (PDB) and read out by PyMOL. All data statistical analyses were performed by Microsoft Office Excel, including deviation and T-test.

2.2 Mammalian hSts-2 Isoforms and Mutants Expression Constructs

The long form hSts-2 cDNA sequence referred to as GenBank reference sequence (NG_029750.1) was obtained from Thermo Fisher. The expression construct was synthesized via PCR-mediated amplification with forward primers that contained a unique restriction enzyme site BamHI and Kozak sequence (5'- TCATTGGATCCGCCGCCACCATGGCAGCGGGG GAGACGCAG -3') and reverse primers that contained FLAG tag coding sequence and a unique restriction enzyme site XhoI (5'- CTGCCTCGAGTCACTTATCGTCATCGTCCTTGTAGTCT CCTCCTCCGTTGCCTGAGATCCAGTTCCTCCA -3'). The reverse primer was purified by PAGE purification (IDT).

The short form hSts-2 cDNA was generated and amplified based on long form constructs by PCR site-directed deletion with primers that contained a codon for aspartic acid (forward primers: 5'- ACGGAAGCATCTCTCTTAGCAGACTGCTCCGTGAAGCCTTGCACC -3', reverse primers: 5'- GGTGCAAGGCTTCACGGAGCAGTCTGCTAAGAGAGATGCTTCCG T -3').

Mutations S18G, R324Q, and D466E were introduced into long form hSts-2 constructs by PCR site-directed mutagenesis (S18G, forward primer: 5'- AAGGTCTCCAACAAG CTCAAGGGCCGCAGCAGTCCCTCGCTCCTG -3', reverse primer 5'- CAGGAGCGAGG GACTGCTGCGGCCCTTGAGCTTGTTGGAGACCTT -3'; R324Q, forward primer: 5'- TG GGTGATTGGGATCTCACAGCAGACGGGCTGCCGGGGCTTCCTG -3', reverse primer: 5'- CAGGAAGCCCCGGGCAGCCCGTCTGCTGTGAGATCCCAATCACCCA -3'; D466E, forward primer: 5'- TTCCAGTCCAGAATTGCAGGGGAGGCGCTACTGGACAGTGGTATC -3', reverse primer: 5'- GATACCACTGTCCAGTAGCGCCTCCCCTGCAATTCTGGACT GGAA -3'). To generate S18G-L28F and S18G-V111M mutants, mutations L28F and V111M were then introduced into S18G long form hSts-2 constructs respectively by PCR site-directed

mutagenesis (L28F, forward primer: 5'- AGTCCCTCGCTCCTGGAGCCCTTCCTGGCC ATGGGCTTCCCGGTG -3', reverse primer: 5'- CACCGGGAAGCCCATGGCCAGGAAG GGCTCCAGGAGCGAGGGACT -3'; V111M, forward primer: 5'- GCTCATGAGGTCTTCC CACACATGACACTCTGTGACTTCTTCACG -3', reverse primer: 5'- CGTGAAGAAGT CACAGAGTGTCATGTGTGGGAAGACCTCATGAGC -3'). Mutants S18G-V111M-R324Q and S18G-D466E were synthesized by digestion and ligation. Short form hSts-2 mutants were generated by subcloning cDNA fragments containing the vitiligo-associated mutations from long form cDNA mutants. The latter group of mutants was generated by Prof. Nick Carpino.

The PCR experiments above were performed with Platinum® *Pfx* DNA polymerase (Invitrogen) following the instructions; the competent *Escherichia.coli* cells for transformation were DH5α cell line from Invitrogen. All of the PCR products above were then purified and subcloned into pBluescript vector for expressing in *Escherichia.coli* and into pCDNA3 vector for expressing in mammalian cells. All PCR products and mutants were confirmed by sequence analysis.

2.3 Cell Culture, Transfection and Jurkat T cells Stimulation

HEK293T cells were grown in DMEM (Giboco) with 10% fetal bovine serum, L-glutamine, pyruvate and penicillin/streptomycin. For transfection, HEK293T cells were plated 24hrs before transfection in the media without penicillin/streptomycin. Jurkat ES-006 cells were cultured in RPMI1640 (Giboco) with 10% fetal bovine serum, L-glutamine and penicillin/streptomycin. Jurkat T cells for transfection were changed into RPMI high glucose media (ref A10491-01) with 10% fetal bovine two or three days before transfection.

To express constructs, HEK293T cells were transiently transfected by Lipofectamine Reagent (Invitrogen) following the optimized protocol based on manufacturer's transfection procedure. For both expression and phosphatase assay, 10μg DNA prepared by QIAGEN Plasmid Maxi Kit and 30μl Lipofectamine Reagent was used for transfection. Cells were cultured in 10cm petri dish, starved for 12hrs after transfection and harvested 48 hrs after transfection. Transiently transfection of Jurkat T cells was performed by electroporation using Ingenio® Electroporation Kits (Mirus) and Nucleofector (Lonza). As mentioned before, Jurkat T cells were passaged with RPMI high glucose media two or three days before transfection at the density of 3.5×10^5 or 2×10^5 cells/ml respectively. 10×10^6 cells and 10μg DNA was used per transfection, additional 0.1μg Renilla and 5μg NFAT-firefly was added for luciferase assay,

other procedures followed Mirus and Lonza instructions. All the plasmids for transfecting Jurkat T cells were prepared by QIAGEN EndoFree Plasmid Maxi Kit. Cells were then plated in 10cm petri dish with 10ml RPMI high glucose media and cultured for 24hrs. For luciferase assay, transfected Jurkat T cells were stimulated 24hrs post-transfection in 96-well U-bottom plates coated with either 30μl/well DPBS (Giboco) or 2μg/ml anti-Human CD3 (OKT3) antibody (eBioscience). Cells were harvested after 8hrs stimulation.

2.4 Cell Lysis, Phosphatase Assay, Immunoprecipitations, and Immunoblots

Lysis buffer containing 50nM Tris, pH7.6, 150mM NaCl, 5mM EDTA, 1mMEGTA and 1% Nonidet P-40 ice-cold before lysing cells. HEK293T cells were washed with cold DPBS once and lysed in 1ml cold lysis buffer. Cell debris was removed by centrifugation. Part of the cell lysates were then mixed with an equal volume of 2x sample buffer for normalization.

For immunoprecipitations and subsequent phosphatase assay, normalized cell lysates were used and mixed with 5μg anti-FLAG rotating at 4℃ for 2hrs, then mixed with 30μl protein A-Sepharose 50% slurry (Sigma) at 4℃ for 1hr. Beads were washed 3x with cold lysis buffer and 3x with room temperature wash buffer containing 25mM HEPES, pH7.2, 50mM NaCl, 5mM DTT, 2.5mM EDTA and 0.1 mg/ml BSA. 10mM substrate 3-*O*-methyfluorescein phosphate (OMFP) was prepared in DMSO storing in -20℃ and 1:20 diluted by wash buffer right before phosphatase assay. Mixed with 100μl 0.5mM OMFP per sample, the beads were then cultured at 37℃ 5 minutes for mouse Sts-1 and 3hrs for other samples. Supernants were transferred into 96-well flat-bottom plates monitoring the dephosphorylation of OMFP by measuring absorbance at 450nm and 477nm using a SpectraMax 190 Microplate reader (Molecular Devices). The value of each sample was the difference of sample value and background value only containing diluted substrate. The final analyses were based on duplicate data that was generated from two independent experiments.

Proteins on the beads were eluted by 2x sample buffer, separated by SDS-PAGE, and transferred to PVDF (Millipore) using a semidry transfer apparatus (Bio-Rad). The PVDFs were then blocked with 3% BSA in Tris-buffered saline (TBS) for 1hr at room temperature, incubated with anti-FLAG at 4℃ for 2hrs. Secondary antibody Alexa Fluor® 680-conjugated goat anti-mouse from Invitrogen were added after washing blots with TBS and incubated either 1hr at room temperature or overnight at 4℃. Washed with TBS, blots were developed with ODYSSEY Infrared Imaging System (LI-COR).

2.5 Luciferase Assay

Luciferase assays were performed with Dual-Luciferase® Reporter Assay kit (Promega). Jurkat T cells were harvested by centrifugation at 4℃, lysed by 1x passive lysis buffer (Promega), frozen at -80℃ and thawed. Cell lysates were then clarified by centrifugation and transferred into Luminate cuvette (BD). Assays were performed in triplicate following the manufacturer's instruction. Luminesence readings of firefly and *Renilla* luciferase activity were measured by Lumat LB 9507 luminometer (EG&G Berthold). NFAT activity was normalized by corresponding basal Renilla luciferase activity. The luciferase assay was performed one time in triplicate.

III. Results

3.1 Expression of human wild-type and mutant Sts-2

To validate the hSts-2 expression constructs that we generated, we chose to express the proteins in HEK293T cells. Firstly, we evaluated the expression level of both the short and long forms of wild-type Sts-2. Cells were cultured in 10cm plates, transfected with 10μg expression vectors or empty vector respectively and harvested following 48hrs in culture. Expression levels were evaluated by anti-Flag immunoblot analysis. As controls, we also transfected murine *Sts-1* and murine *Sts-2* (corresponds to short form hSts-2). Figure 3.1 demonstrates that both hSts-2 short form and hSts-2 long form express well in HEK293T cells. Interestingly, the expression level of short form hSts-2 is much higher than the level of long form hSts-2. Additionally, human short form Sts-2 also expresses to a much higher level than its murine orthologue (Figure 3.1a). Slow migrating bands were easily observed in all of the cell lysates transfected with Sts except long form hSts-2. We considered those bands were mono-ubiquitinated Sts-2[32]. We then evaluated the expression levels of the Sts-2 alleles containing the vitiligo-associated mutations. We observed that all the mutants of both the short and long forms of hSts-2 expressed to the same level as wild type hSts-2 (Figure 3.1b, c).

3.2 Effect of vitiligo-associated mutations on Sts-2 phosphatase activity

It has been shown that murine Sts-2 has *in vitro* phosphatase activity associated with its C-terminal PGM domain [30]. To determine the phosphatase activity of human wild-type Sts-2, *in vitro* immune complex phosphatase assays were performed using OMFP as substrate. Early research confirmed high phosphatase activity of mSts-1 *in vitro*, thus mSts-1 served as a positive control. Consistent with previous results, we observed a significant difference between the catalytic activities associated with mSts-1 and mSts-2 (Figure 3.2). We also observed that the two isoforms of human Sts-2 had significantly reduced *in vitro* phosphatase activity relative to mSts-1. Indeed, both the short and long forms of human Sts-2 displayed lower activity than murine Sts-2. The phosphatase activity of Sts-2 is thought to be important for its *in vivo* functions [30], although it is currently unclear whether there are intracellular regulatory mechanisms that increase Sts-2 catalytic activity.

We then evaluated phosphatase activities of the various Sts-2 vitiligo-associated alleles relative to wild-type Sts-2, utilizing OMFP as an *in vitro* substrate. No significant differences

were observed between the catalytic activities of wild-type hSts-2 and the different mutants (Figure 3.3-3.4).

3.3 Effect of vitiligo-associated mutations on Sts-2 function downstream of the TCR.

To assess the effects of vitiligo-associated mutations on Sts-2 function, we chose to employ a T cell line over-expression system. Specifically, to evaluate the effects of Sts-2 on TCR signaling pathways, it was co-expressed in Jurkat T cells with a Nuclear factor of activated T cells (NFAT) - luciferase reporter construct. NFAT is a transcription factor whose level of activation following TCR engagement is critically and directly dependent on the overall strength of activation of signaling pathways downstream of the TCR. Over-expression of wild-type Sts-1 in Jurkat T cells leads to a reduced NFAT response following TCR stimulation, consistent with the role of Sts-1 as a negative regulator of TCR signaling. Interestingly, it has been published that over-expression of human short form Sts-2 in Jurkat T cells leads to *increased* NFAT activation following TCR stimulation [28]. Independent experiments in our laboratory have previously indicated that *murine* short form Sts-2 also leads to increased NFAT activation following over-expression in Jurkat T cells [San Luis and Carpino, unpublished data]. These results are not consistent with the simple hypothesis that Sts-2 is a negative regulator of TCR signaling, a hypothesis that emerged from analyzing the properties of *Sts-2*$^{-/-}$ T cells. This contradiction has not been resolved. Nonetheless, because over-expression of Sts-2 has a clear effect on TCR signaling pathways in Jurkat T cells, we utilized the Jurkat over-expression system to assess the effects of vitiligo-associated mutations on Sts-2 function.

Consistent with published results, and our laboratory's unpublished observations, we observed that mSts-1 over-expression led to diminished NFAT activation and mSts-2 over-expression led to enhanced NFAT activation (Figure 3.5). Interestingly, over-expression of short form hSts-2 also led to NFAT activation that is significantly enhanced relative to mSts-2 but over-expression of long form hSts-2 resulted in reduced NFAT activation. Thus, the short and long forms of Sts-2 appear to different functions and possibly different mechanisms of action.

We then investigated the effects of specific point mutations within Sts-2 on NFAT activation. We observed that the vitiligo-associated mutations within either short or long form Sts-2 did not have an appreciable effect on Sts-2 function in the context of this assay. That is to say, over-expression of mutants of short form Sts-2 led to increased NFAT activation (similar to wild-type short form Sts-2), while over-expression of mutants of long form Sts-2 led to reduced

NFAT activation (similar to wild-type long form Sts-2) (Figure 3.6-3.7). However, it is important to point out the following caveat: the luciferase assays of long form hSts-2 mutants were easily reproduced and consistent, whereas it was more difficult to get reproducibly consistent luciferase assay data when the effects of the short form hSts-2 mutants were evaluated. Although the data presented in Figure 3.6 was repeated twice for a total of three experiments, there was a great deal of variability in our results. For example, in one experiment, hSts-2s S18G-V111M up-regulated NFAT activity relative to wild-type short form hSts2, while in another experiment we obtained the opposite result. Likewise, we also obtained inconsistent results with the S18G, and S18G-L28F mutants.

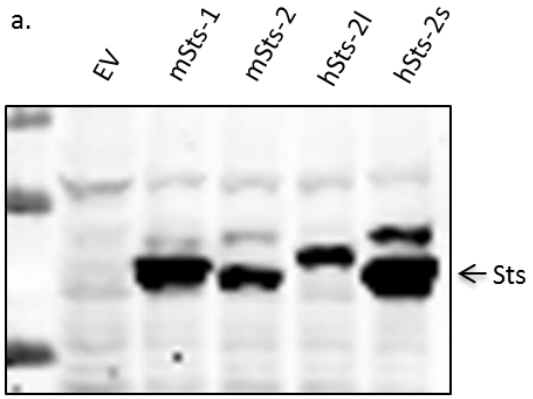
a.
EV
mSts-1
mSts-2
hSts-2l
hSts-2s
Sts
WB: anti-Flag

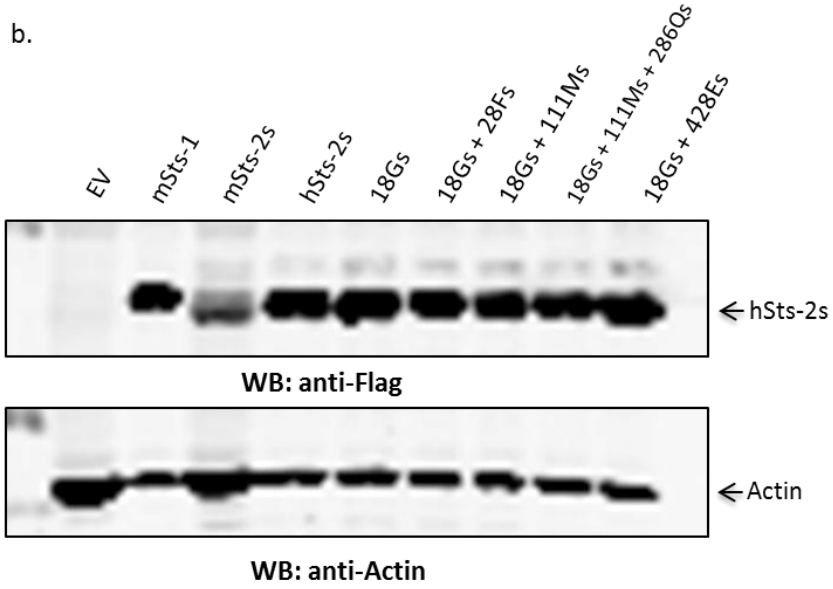
b.
EV
mSts-1
mSts-2s
hSts-2s
18Gs
18Gs + 28Fs
18Gs + 111Ms
18Gs + 111Ms + 286Qs
18Gs + 428Es
hSts-2s
WB: anti-Flag
Actin
WB: anti-Actin

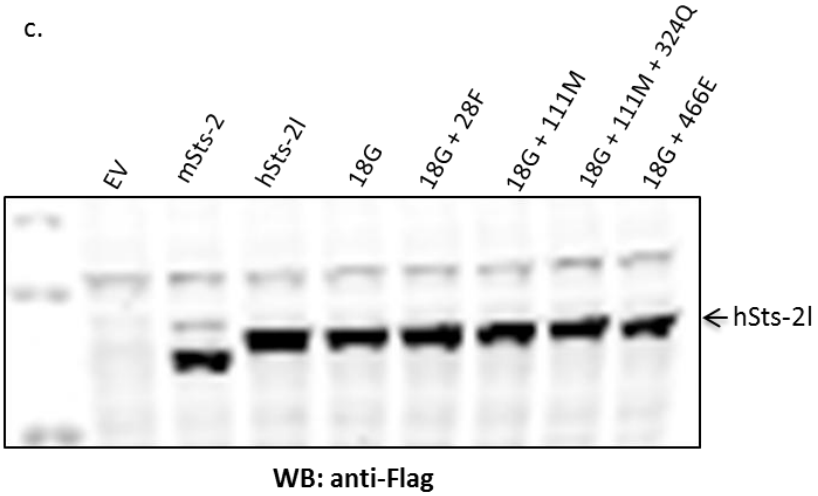
c.
EV
mSts-2
hSts-2l
18G
18G + 28F
18G + 111M
18G + 111M + 324Q
18G + 466E
hSts-2l
WB: anti-Flag

Figure 3.1: Expression of hSts-2 wild-type and vitiligo-associated mutants in HEK293T cells.

293T cells were transfected with the indicated expression constructs, harvested, and analyzed by SDS-PAGE/immunoblot analysis. (a) Expression of the indicated wild-type Sts isoforms. (b) Expression of short form hSts-2 mutants. (c) Expression of long form hSts-2 mutants.

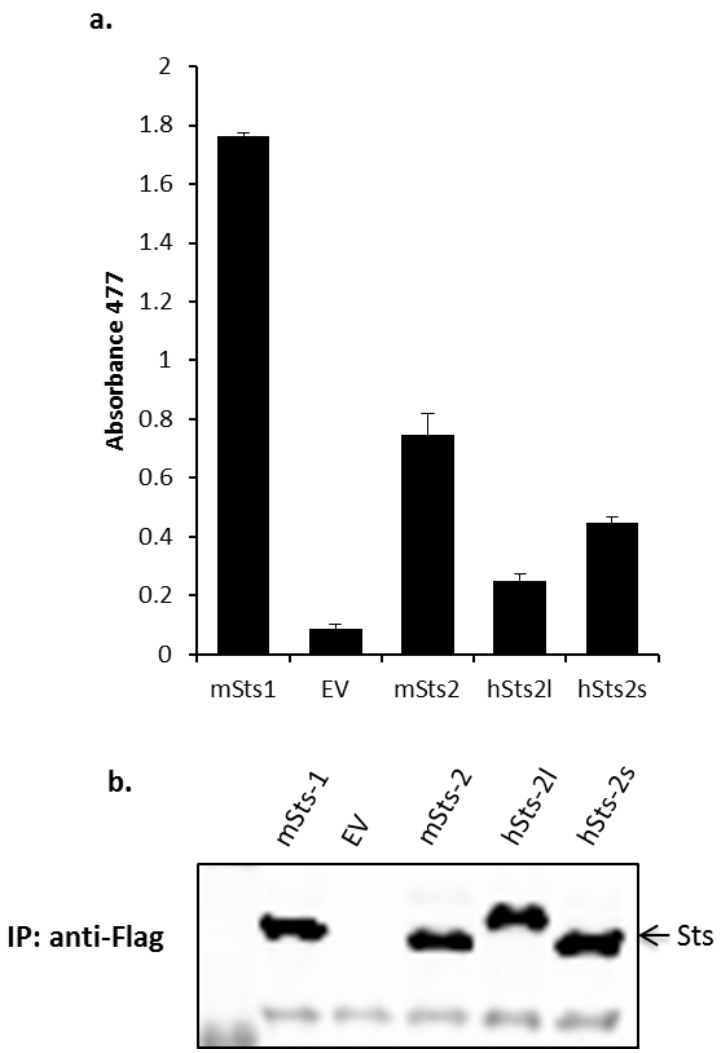

Figure 3.2: Phosphatase activity of hSts-2 wild-types *in vitro*.

Wide type Sts-2 proteins were expressed by transient transfection of 293T cells and isolated by anti-FLAG immunoprecipitation. *In vitro* immune complex assays were performed using OMFP as substrate, with mSts-1 a positive control (a) Phosphatase activity determined by absorbance of products at 477nm shows the relative lower phosphatase activity of long form and short form hSts-2 comparing to the weak phosphatase activity of mouse Sts-2. The activity of long form hSts-2 is approximately 50% lower than that of short form hSts-2. (b) Levels of protein in each assay were assessed by immunoblot analysis.

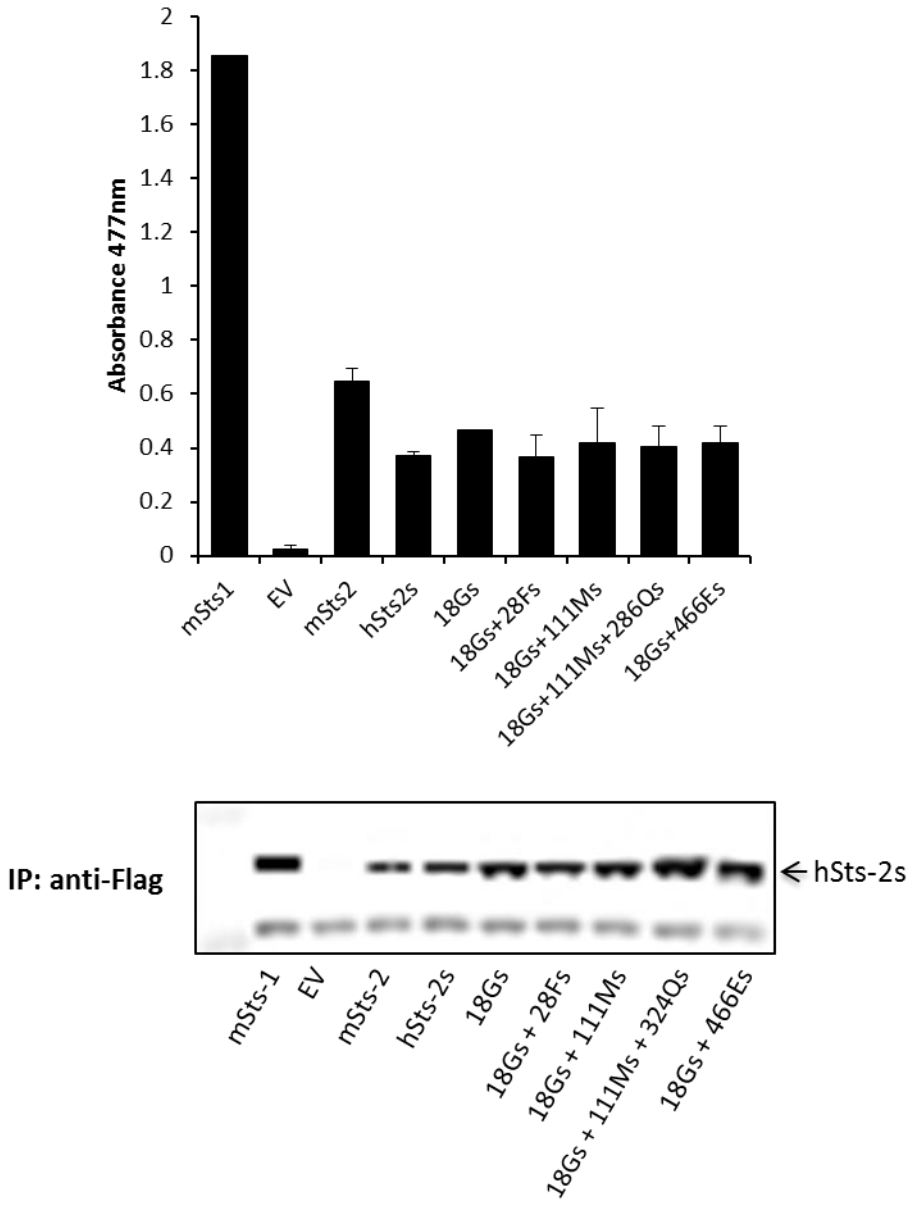

Figure 3.3: Phosphatase activity of short form hSts-2 mutants *in vitro*.

Phosphatase assay were performed as described in Figure 3.2. Results shows similar phosphatase activity of short form mutants comparing to each other and wild-type short form hSts-2.

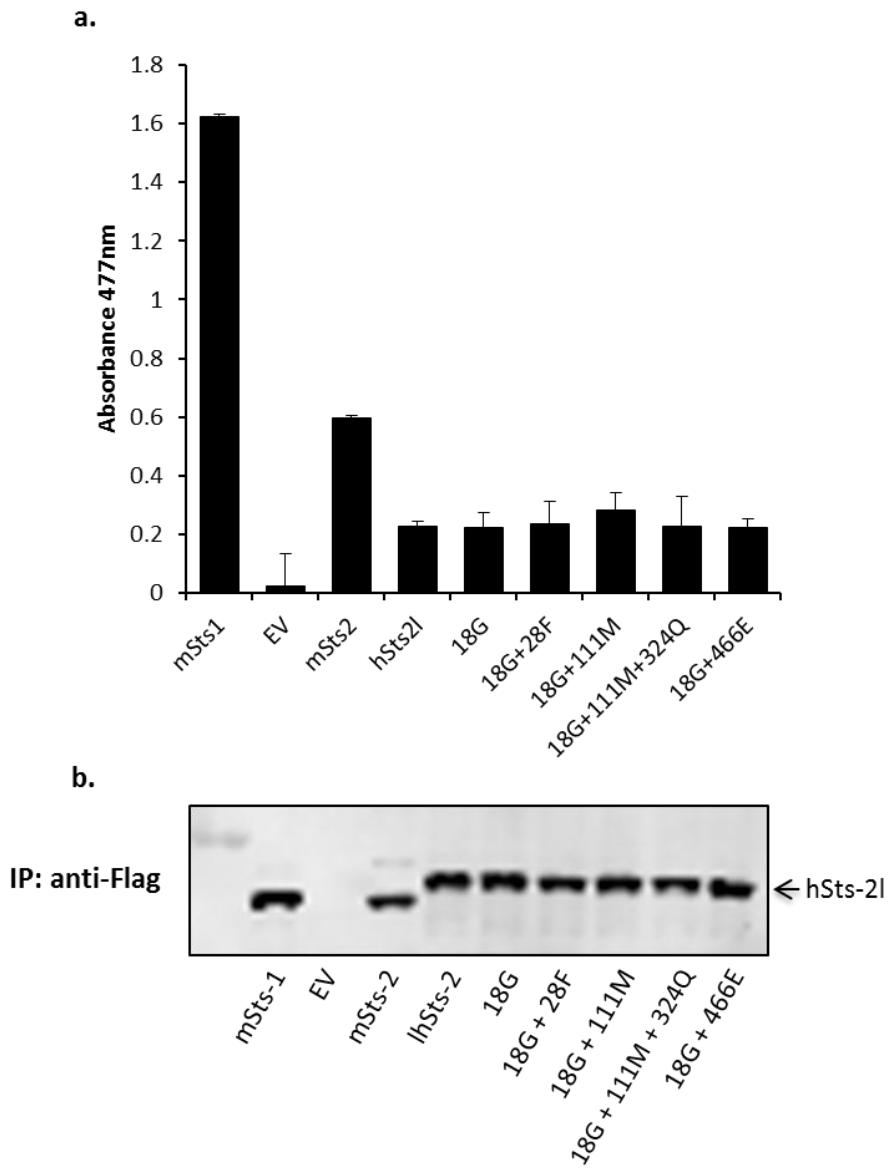

Figure 3.4: Phosphatase activity of long form hSts-2 mutants *in vitro*.

Phosphatase assay were performed as described in Figure 3.2. Results shows similar phosphatase activity of long form mutants comparing to each other and wild-type long form hSts-2.

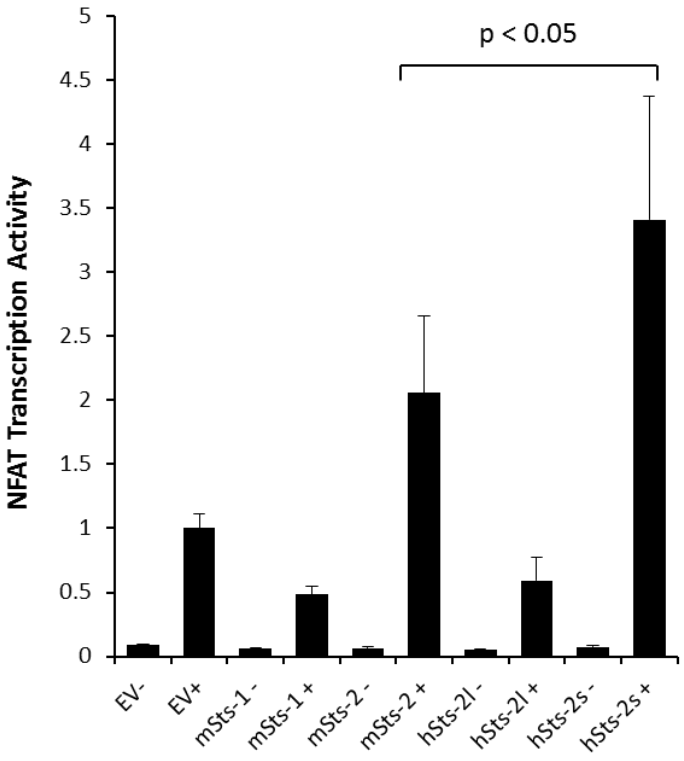

Figure 3.5: Effect of Sts-2 on TCR signaling pathways.

For analysis of TCR signaling, Sts expression vectors and luciferase reporter vectors were co-transfected into Jurkat T cells and stimulated with anti-CD3. Cells were harvested after 8hrs stimulation and prepared for luciferase assay. Empty vector was used as basal level control while mouse Sts-1 was used as positive control.

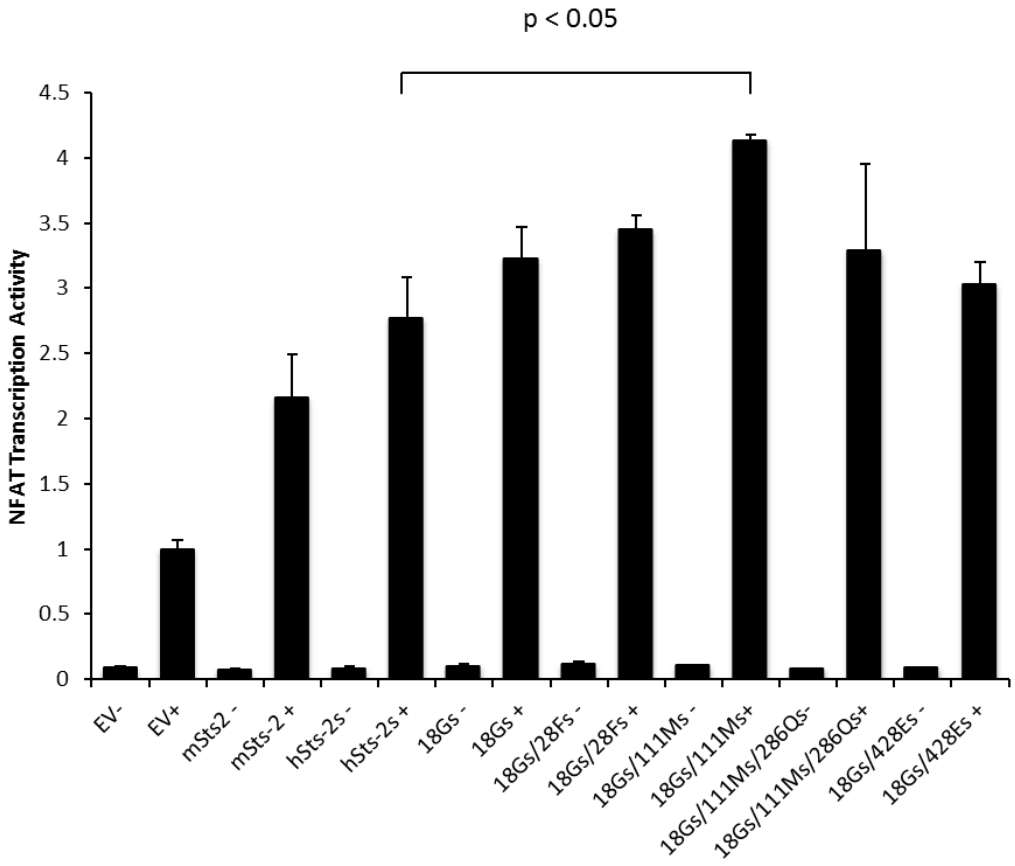

Figure 3.6: Effect of short form Sts-2 vitiligo-associated mutants on TCR signaling pathways.

Luciferase assays were performed as described in Figure 3.5.

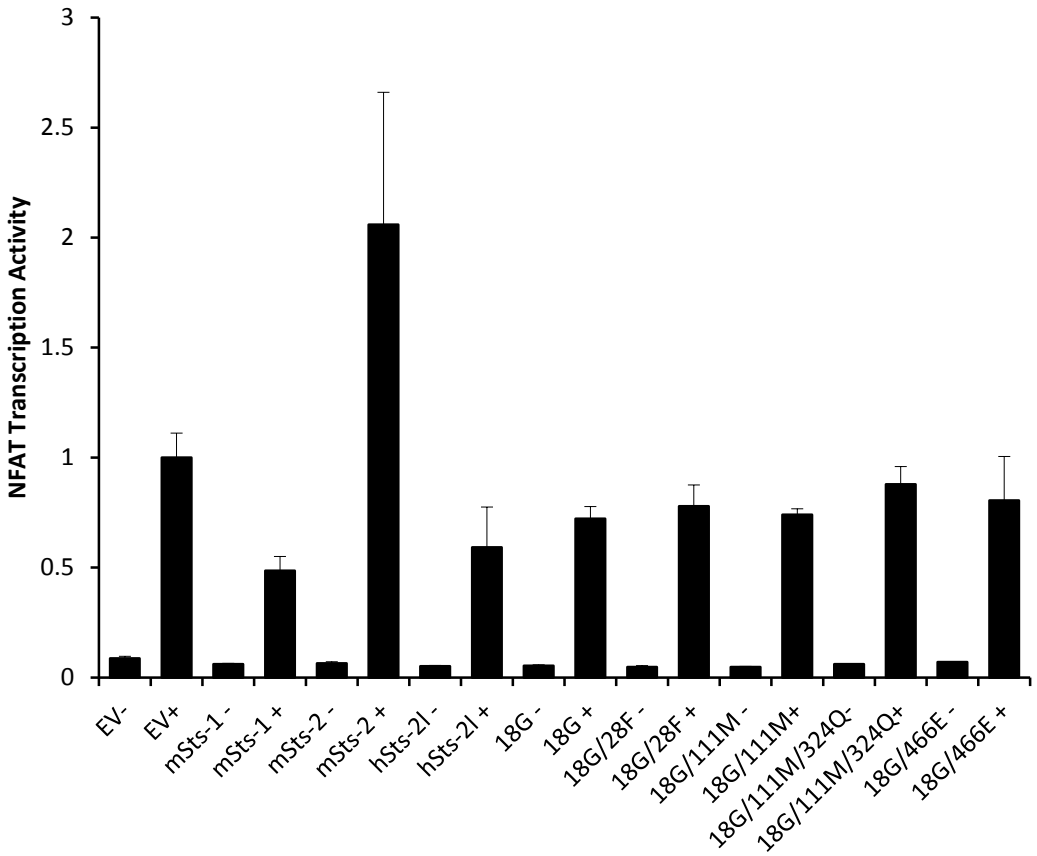

Figure 3.7: Effect of long form Sts-2 vitiligo-associated mutants on TCR signaling pathways.

Luciferase assays were performed as described in Figure 3.5. Cells with over-expressed long form hSts-2 mutants perform a similar TCR activity to wild-type.

IV. Discussion

The study presented here consisted of two parts. Firstly, we evaluated similarities and differences between the short form and long form of human Sts-2. Secondly, we evaluated the effects of specific mutations on Sts-2 function. The mutations were identified in a genome-wide association study that sought to identify molecular determinants of the disease vitiligo. Thus, this study is one of the first functional analyses of Sts-2 in the context of disease.

There are many puzzling aspects concerning the mutations that were presented by Jin Y. *et al.* In some cases, one can easily envision how they might be deleterious to the function of Sts-2, while in other cases it is not so clear. For example, regarding the S18G allele, it is unclear why this particular mutation always appears in combination with additional mutations. Ser-18 is not contained within any of the defined domains that make up the Sts-2 proteins. Rather, it is in the short N-terminal region preceding the UBA domain. Interestingly, the corresponding residue in mSts-2 is a glycine. Among the five mutants, L28F is the only mutation that targets a highly conserved residue. It is easy to assume that L28F may affect the stabilization of UBA domain as the conserved residue is in the hydrophobic core. Val-111 is located beside the potential PDE domain catalytic residue His-110; thus, mutation of Val-111 to methionine could have an effect on PDE enzymatic activity, although the function of the PDE domain in Sts-2 is still unclear. Another two mutants are located neither in conserved motif nor catalytic motif. Arg-324 is located in the SH3 domain, but on the opposite side of the domain from the ligand binding region. Indeed, the corresponding sites in other SH3 domains are variable. The residue Asp-466 in the mSts-1, mSts-2, and hSts-1 corresponds to a glutamic acid. Considering the residue is located on the opposite side of the molecule from the active site, one of the questions is that whether or not the change of aspartic acid into glutamic acid would affect PGM domain function.

Our study reveals that both human Sts-2 isoforms have weaker *in vitro* phosphatase activity than mouse Sts-2, although mSts-2 and short form hSts-2 are highly similar in sequence. Considering 17% of the amino acids are different between the orthologues, there may be slight differences in their individual structures that could account for the observed differences in activities. It is interesting that long form hSts-2 has lower phosphatase activity than short form, although the reason for this difference is currently unclear. All of the vitiligo-derived mutants appear to possess similar phosphatase activity as their wild-type counterparts, suggesting that if the vitiligo mutations impair Sts-2 function, it is not by directly altering phosphatase activity.

However, it is also possible that the point mutations present in other domains could influence the manner in which the PGM domain interacts with intracellular substrates *in vivo,* thereby affecting phosphatase activity indirectly. Finally, it is important to keep in mind that our *in vitro* observations may not have direct relevance to the *in vivo* situation where Sts-2 encounters its natural substrates.

The most interesting finding in this study is the functional differences we observed between the long and short forms of hSts-2. Specifically, with regards to our over-expression studies utilizing Jurkat T cells, we observed that cells expressing human Sts-2 short form are hyper-activated following TCR stimulation, while those expressing human Sts-2 long form are hypo-activated. These differences could be due to the fact that Sts-2 has multi-faceted functions. One of the possibilities is that long form and short form may target different proteins. For example, only short form Sts-2 binds to the ZAP-70 negative regulator c-Cbl by its SH3 domain and facilitates c-Cbl ubiquitination directly or indirectly through its UBA domain [28]; in contrast, the long form may expose different binding residues as it has a larger PDE domain and bind to other proteins, thereby stimulating negative regulators or repressing positive regulators. Another possibility is that long form Sts-2 acts as a dominant negative regulator of the short form. It may target the short form directly by dimerization via the C-terminal PGM domain, allowing for the inhibition of short form Sts-2. In this scenario, overexpression of long form Sts-2 would suppress short form Sts-2-mediated c-Cbl ubiquitination and down-regulate T cell signaling. Notably, overexpression of long form Sts-2 in Jurkat T cells results in a reduction of NFAT activation similar to levels observed when Sts-1 is over-expressed, consistent with the hypothesis that Sts-2 negatively regulates TCR signaling [26]. Additionally, the domain between the UBA and SH3 domains where the alternative splice site is located has not been studied yet. The Sts-2 PDE-like domain may regulate T cell signaling through some unique manner that has not been uncovered. For example, it may be involved in protein-protein interaction for recruiting other proteins, or it may stimulate certain substrates by phosphodiesterase activity. In such a case, a reasonable explanation could be that long form Sts-2 has an active PDE domain down-regulating signaling and influencing the activities of other domains. One can also imagine a scenario in which long form Sts-2 cannot bind to and negatively regulate the negative regulator c-Cbl, so that overexpression of long form Sts-2 would then down-regulate TCR downstream signaling; in contrast, the short form, with its ability to interact with Cbl, might have the opposite effect on

Cbl, which would lead to an opposite outcome. The contradictory results obtained when two Sts-2 isoforms are expressed in Jurkat T cells suggests that understanding the relation between long form and short form Sts-2 is significant for understanding how Sts-2 regulates TCR signaling pathways. Thus, further functional analysis of the two forms of hSts-2 is warranted.

In our assays, we did not find a clear difference between the functions of wild-type Sts-2 and the Sts-2 alleles with the vitiligo-associated mutations. Given that the stimulation time was 8 hours, one potential reason is that early TCR signaling events are altered but have been compensated for following 8 hours stimulation. In the context of generalized vitiligo, it is also possible that Sts-2 is involved the development of the disease through the TCR-independent apoptosis pathways. In particular, the mutants may affect the recruitment of caspase-independent apoptosis factor AIF and other proteins leading to an elevated level of T cells in affected area and enhancement of T cell-induced melanocytes apoptosis [31]. Thus, the effects of vitiligo-associated mutations in Sts-2 are still unclear. Therefore, further functional analysis is warranted to identify their impact on Sts-2 functions. One important experimental condition that could be altered is varying the time length of TCR stimulation. Another avenue of investigation includes evaluating the potential role of the vitiligo-associated mutations on Sts-2 intracellular localization.

References

1. Abbas A, Lichtman A, Pillai S. (2007) Cellular and molecular immunology. Saunders Elsevier, Philadelphia, PA, 6 edn.
2. Murphy K. (2011) Janeway's immunobiology. Garland Science, New York, NY, 8 edn.
3. Singer AL, Koretzky GA. (2002) Control of T cell function by positive and negative regulators. Science. 296(5573):1639-40.
4. Smith-Garvin JE, Koretzky GA, Jordan MS. (2009) T cell activation. Annu Rev Immunol. 27:591-619.
5. Choudhuri K, Dustin ML. (2010) Signaling microdomains in T cells. FEBS Lett. 584(24):4823-31.
6. Fooksman DR, Vardhana S, Vasiliver-Shamis G *et al*. (2010) Functional anatomy of T cell activation and synapse formation. Annu Rev Immunol. 28:79-105.
7. Varma R, Campi G, Yokosuka T *et al*. (2006) T cell receptor-proximal signals are sustained in peripheral microclusters and terminated in the central supramolecular activation cluster. Immunity. 25(1):117-27.
8. Müller MR, Rao A. (2010) NFAT, immunity and cancer: a transcription factor comes of age. Nat Rev Immunol. 10(9):645-56.
9. Paolino M, Penninger JM. (2010) Cbl-b in T-cell activation. Semin Immunopathol. 32(2):137-48.
10. Vang T, Abrahamsen H, Myklebust S *et al*. (2004) Knockdown of C-terminal Src kinase by siRNA-mediated RNA interference augments T cell receptor signaling in mature T cells. Eur J Immunol. 34(8):2191-9.
11. Naramura M, Jang IK, Kole H *et al.* (2002) c-Cbl and Cbl-b regulate T cell responsiveness by promoting ligand-induced TCR down-modulation. Nat Immunol. 3(12):1192-9.
12. Teft WA, Kirchhof MG, Madrenas J. (2006) A molecular perspective of CTLA-4 function. Annu Rev Immunol. 24:65-97.
13. Ribon V, Herrera R, Kay BK *et al.* (1998) A role for CAP, a novel, multifunctional Src homology 3 domain-containing protein in formation of actin stress fibers and focal adhesions. J Biol Chem. 273(7):4073-80.
14. Rezaei N, Gavalas NG, Weetman AP *et al*. (2007) Autoimmunity as an aetiological factor in vitiligo. J Eur Acad Dermatol Venereol. 21(7):865-76.
15. Spritz RA. (2012) Six decades of vitiligo genetics: genome-wide studies provide insights into autoimmune pathogenesis. J Invest Dermatol. 132(2):268-73.
16. Jin Y, Birlea SA, Fain PR *et al*. (2010) Variant of TYR and autoimmunity susceptibility loci in generalized vitiligo. N Engl J Med. 362(18):1686-97.
17. Firooz A, Bouzari N, Fallah N *et al*. (2004) What patients with vitiligo believe about their condition. Int J Dermatol. 43(11):811-4.
18. van den Wijngaard RM, Aten J, Scheepmaker A *et al*. (2000) Expression and modulation of apoptosis regulatory molecules in human melanocytes: significance in vitiligo. Br J Dermatol. 143(3):573-81.
19. Schallreuter KU, Behrens-Williams S, Khaliq TP *et al*. (2003) Increased epidermal functioning wild-type p53 expression in vitiligo. Exp Dermatol. 12(3):268-77.
20. Ogg GS, Rod Dunbar P, Romero P *et al*. (1998) High frequency of skin-homing melanocyte-specific cytotoxic T lymphocytes in autoimmune vitiligo. J Exp Med. 188(6):1203-8.

21. Lang KS, Caroli CC, Muhm A *et al*. (2001) HLA-A2 restricted, melanocyte-specific CD8(+) T lymphocytes detected in vitiligo patients are related to disease activity and are predominantly directed against MelanA/MART1. J Invest Dermatol. 116(6):891-7.
22. Lili Y, Yi W, Ji Y *et al*. (2012) Global activation of CD8+ cytotoxic T lymphocytes correlates with an impairment in regulatory T cells in patients with generalized vitiligo. PLoS One. 7(5):e37513.
23. Oyarbide-Valencia K, van den Boorn JG, Denman CJ *et al*. (2006) Therapeutic implications of autoimmune vitiligo T cells. Autoimmun Rev. 5(7):486-92.
24. Jin Y, Ferrara T, Gowan K *et al*. (2012) Next-generation DNA re-sequencing identifies common variants of TYR and HLA-A that modulate the risk of generalized vitiligo via antigen presentation. J Invest Dermatol. 132(6):1730-3.
25. Carpino N, Kobayashi R, Zang H *et al*. (2002) Identification, cDNA cloning, and targeted deletion of p70, a novel, ubiquitously expressed SH3 domain-containing protein. Mol Cell Biol. 22(21):7491-500.
26. Carpino N, Turner S, Mekala D *et al*. (2004) Regulation of ZAP-70 activation and TCR signaling by two related proteins, Sts-1 and Sts-2. Immunity. 20(1):37-46.
27. Weil R, Israël A. (2006) Deciphering the pathway from the TCR to NF-kappaB. Cell Death Differ. 13(5):826-33.
28. Feshchenko EA, Smirnova EV, Swaminathan G *et al*. (2004) TULA: an SH3- and UBA-containing protein that binds to c-Cbl and ubiquitin. Oncogene. 23(27):4690-706.
29. Mikhailik A, Ford B, Keller J *et al*. (2007) A phosphatase activity of Sts-1 contributes to the suppression of TCR signaling. Mol Cell. 27(3):486-97.
30. San Luis B, Sondgeroth B, Nassar N *et al*. (2011) Sts-2 is a phosphatase that negatively regulates zeta-associated protein (ZAP)-70 and T cell receptor signaling pathways. J Biol Chem. 286(18):15943-54.
31. Collingwood TS, Smirnova EV, Bogush M *et al*. (2007) T-cell ubiquitin ligand affects cell death through a functional interaction with apoptosis-inducing factor, a key factor of caspase-independent apoptosis. J Biol Chem. 282(42):30920-8.
32. Kowanetz K, Crosetto N, Haglund K *et al*. (2004) Suppressors of T-cell receptor signaling Sts-1 and Sts-2 bind to Cbl and inhibit endocytosis of receptor tyrosine kinases. J Biol Chem. 279(31):32786-95.
33. Plagnol V, Howson JM, Smyth DJ *et al*. (2011) Genome-wide association analysis of autoantibody positivity in type 1 diabetes cases. PLoS Genet. 7(8):e1002216.
34. Zhernakova A, Stahl EA, Trynka G *et al*. (2011) Meta-analysis of genome-wide association studies in celiac disease and rheumatoid arthritis identifies fourteen non-HLA shared loci. PLoS Genet. 7(2):e1002004.
35. Kozlov G, Nguyen L, Lin T *et al*. (2007) Structural basis of ubiquitin recognition by the ubiquitin-associated (UBA) domain of the ubiquitin ligase EDD. J Biol Chem. 282(49):35787-95.
36. Nguyen JT, Turck CW, Cohen FE *et al*. (1998) Exploiting the basis of proline recognition by SH3 and WW domains: design of N-substituted inhibitors. Science. 282(5396):2088-92.
37. Ding F, Dokholyan NV, Buldyrev SV *et al*. (2002) Molecular dynamics simulation of the SH3 domain aggregation suggests a generic amyloidogenesis mechanism. J Mol Biol. 324(4):851-7.

38. Chen Y, Jakoncic J, Parker KA *et al*. Structures of the phosphorylated and VO(3)-bound 2H-phosphatase domain of Sts-2. Biochemistry. 48(34):8129-35.
39. Peschard P, Kozlov G, Lin T *et al*. (2007) Structural basis for ubiquitin-mediated dimerization and activation of the ubiquitin protein ligase Cbl-b. Mol Cell. 27(3):474-85.
40. Williams BL, Schreiber KL, Zhang W *et al*. (1998) Genetic evidence for differential coupling of Syk family kinases to the T-cell receptor: reconstitution studies in a ZAP-70-deficient Jurkat T-cell line. Mol Cell Biol. 18(3):1388-99.
41. Kozlov G, Peschard P, Zimmerman B *et al*. (2007) Structural basis for UBA-mediated dimerization of c-Cbl ubiquitin ligase. J Biol Chem. 282(37):27547-55.
42. Mazumder R, Iyer LM, Vasudevan S *et al*. (2002) Detection of novel members, structure-function analysis and evolutionary classification of the 2H phosphoesterase superfamily. Nucleic Acids Res. 30(23):5229-43.
43. Levy I, Horvath A, Azevedo M et al. (2011) Phosphodiesterase function and endocrine cells: links to human disease and roles in tumor development and treatment. Curr Opin Pharmacol. 11(6):689-97.